SIMULATION OF DAYLIGHT PERFORMANCE OF BUILDINGS BY THE DAYLIGHT SOURCE MODEL BASED ON GEOSTATIONAL METEOROLOGICAL SATELLITE IMAGES

Yoshiaki Uetani
Fukuyama University, Department of Architecture
Fukuyama 729-0292, JAPAN

ABSTRACT

This paper introduces a method to simulate the daylight performance of buildings using geostational meteorological satellite images. A new statistical method enables to estimate global and direct solar irradiance values at hourly intervals by the pixel values of satellites images. Luminous efficiency functions convert the global and direct irradiance values into diffuse and direct daylight illuminance values. The daylight source model is combined with a daylight calculation program to calculate spatial and temporal distributions of illuminance and luminance. As a result, the daylight performance of buildings is able to be estimated in various weather conditions at any location and time.

INTRODUCTION

To design an architecture with energy efficiency and luminous environment of good quality, daylighting simulation methods and fundamental daylight availability data for various weather conditions are essential. Although a number of numerical models on dayligting and solar radiation have been developed on various sky conditions, these study are usually based on the measured data by surface observations of the sky at the limited number of daylighting and meteorological observatories in the world. Because of the financial difficulty to set up and operate such a station, daylight availability raw data incline to cities and countries where major research institutes are located.

As alternative approaches of surface observations, researchers have developed statistical models [1] and physical models [2] to estimate the insolation data by meteorological satellite images. The statistical approaches have been developed to be a major project [3,4]. The satellite-derived irradiance has been applied to simulations of solar energy system [5] and daylighting [6].

The author has recently developed a new statistical model for global and direct irradiance using the images of Japanese geostational meteorological satellite GMS-5 [7]. The irradiance values are converted into diffuse and direct illuminance values by the luminous efficiency functions. The model is combined with a daylighting simulation program to simulate daylighting performance of buildings. The system is capable of simulating spatial and temporal distribution of illuminance and luminance in building environments.

METHODOLOGY

Geostational Meteorological Satellite

There are five geostational meteorological satellites above the equator observing the globe: METEOSAT (0˚E), GOMS (76˚E), GMS (140˚E), GOES (135˚W) and GOES (75 ˚W). Two polar orbiting meteorological satellites, NOAA and METEOR are also in operation. In this paper, the images observed by the Japanese geostational meteorological satellite GMS-5 are utilized. GMS-5, nicknamed 'HIMAWARI' or sunflower in Japanese, is stationary at the altitude of 35800 kilometers above the equator, 140 degrees of east longitude.

The Visible and Infrared Spin Scan Radiometer (VISSR) carried by GMS-5 is composed of three infrared sensors (IR1 channel: 10.5~11.5 μm, IR2 channel: 11.5~12.5 μm, IR3 channel: 6.5~7.5 μm) and an array of four visible sensors (VIS channel: 0.50~0.75 μm). GMS-5 scans the globe from the North Pole to the South Pole in 25 minutes every hour. The visual sensor array captures an image of 13376 x 10000 pixels with 6 bit depth. Each of the infrared sensors captures an image of 6688 x 2500 pixels with 8 bit depth. The resolutions on the surface right under the GMS-5 are 1.25km/pixel for the visual sensor array and 5km/pixel for each of the infrared sensors. The captured VISSR signals are transferred to Commanding and Data Acquisition Center (CDAS) located in a suburb of Tokyo, and provided for weather forecasts and other applications.

Visible image (VIS channel) provides us a view of the earth close to the human senses with the highest spatial resolution [8] (**Figure 1**). Each pixel of the visible image is converted into the albedo by the calibration data (**Figure 4**) provided with the image.

Infrared image (IR1 channel) is the most familiar image on weather forecast programs (**Figure 2**). Each pixel is converted into the equivalent black body temperature by the provided calibration data (**Figure 5**). The temperature by the infrared image corresponds to the cloud height as the atmosphere cools with height. Infrared images are usually inverted so that the colder clouds appear brighter and the warmer land and sea appear darker as in visible images.

Water vapor image (IR3 channel) represents the radiation in water vapor absorption bands. The image (**Fig-**

ure 3) shows the highest clouds but swirls covers lands and seas. Each pixel is converted into the equivalent black body temperature distributions by the provided calibration data (**Figure 5**) as IR1 channel.

In the following regression analysis, off-line data of VISSR images [8] are utilized. The coordinate transformation of the globe images produces square images surrounded by two pairs of latitudes (20˚N and 50˚N) and longitudes (120˚E and 150˚E). VIS, IR1, and IR3 channels are referred as VS, IR, and WV images respectively.

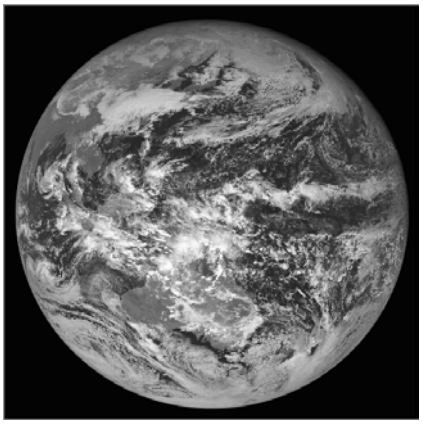

Figure 1 VIS channel (Visible)

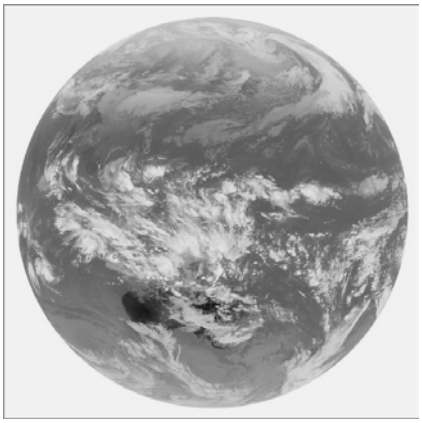

Figure 2 IR1 channel (Split window)

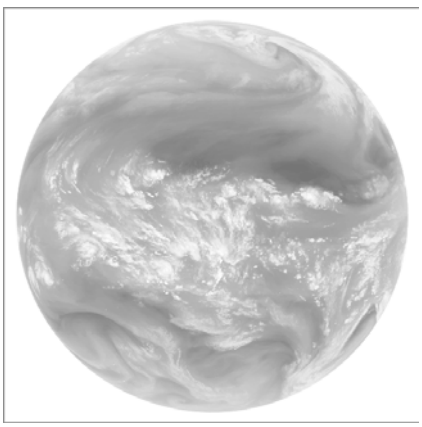

Figure 3 IR3 channel (Water vapour)

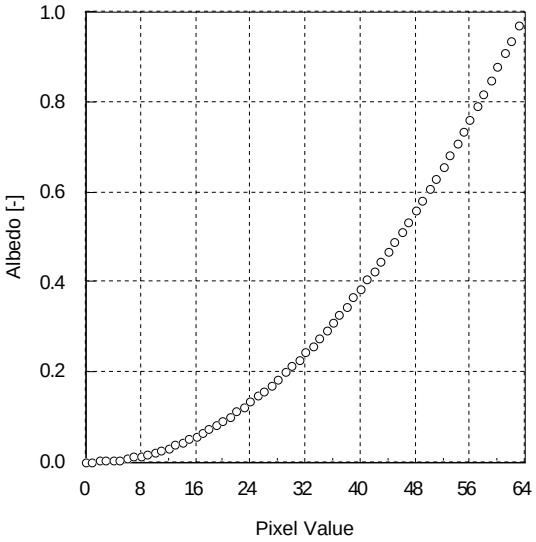

Figure 4 Calibration data for VIS(VS) image

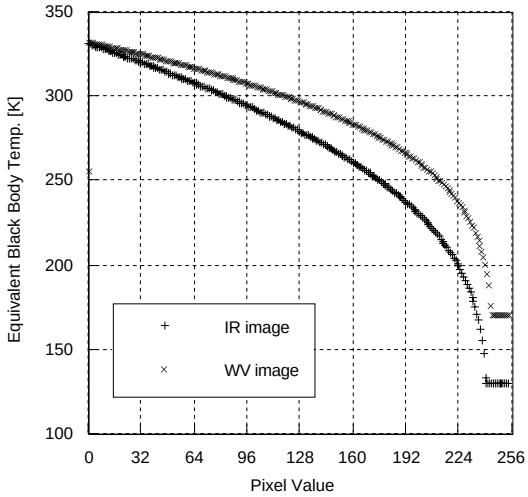

Figure 5 Calibration data for IR1(IR) and IR3(WV) images

Multiple Regression Models of global and direct irradiance [7]

A multiple linear regression analysis was performed to predict the surface observed global and direct irradiance values from the satellite observed VS, IR, and WV image values. For the surface observed hourly cumulative global irradiance I_{oG} [MJ/m²] and direct normal irradiance I_{oDN} [MJ/m²], the observed data at the Fukuoka Meteorological Observatory (130˚23'E, 33˚35'N) from July 1, 1996 to June 30, 1997 are utilized. The cloud amount c_o visually observed every 3 hours at the observatory are used as supplementary data in the analysis. The surface observed hourly cumulative direct horizontal irradiance I_{oDH} [MJ/m²] was derived from the direct normal irradiance I_{oDN} and the solar elevation angle h_s .

For the satellite observed images, the off-line data of VISSR images with calibration data [9] are utilized as mentioned above. The resolution of the satellite im-

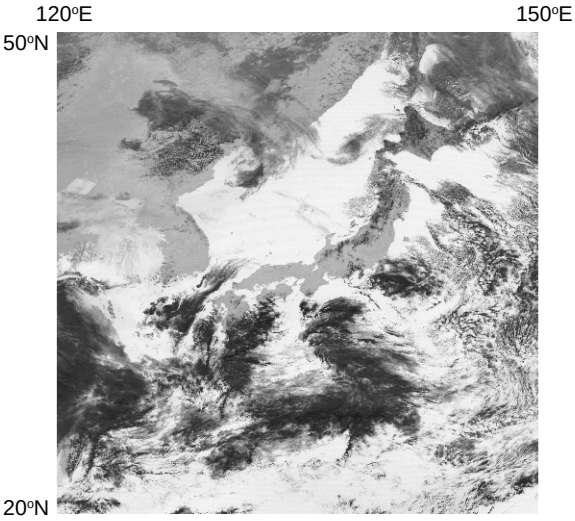

Figure 6 VS image around Japan scanned from 11:34:25AM to 11:39:16AM on March 18, 1997

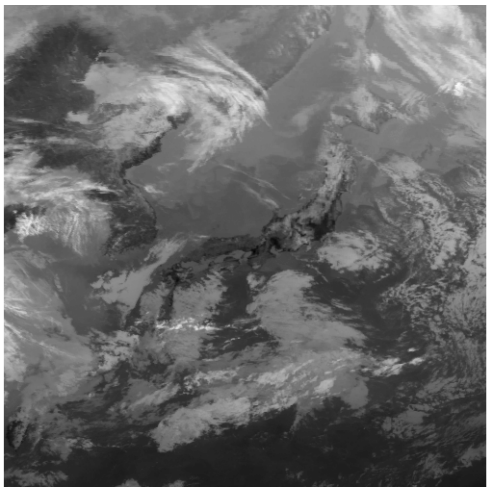

Figure 7 IR image around Japan scanned from 11:34:25AM to 11:39:16AM on March 18, 1997

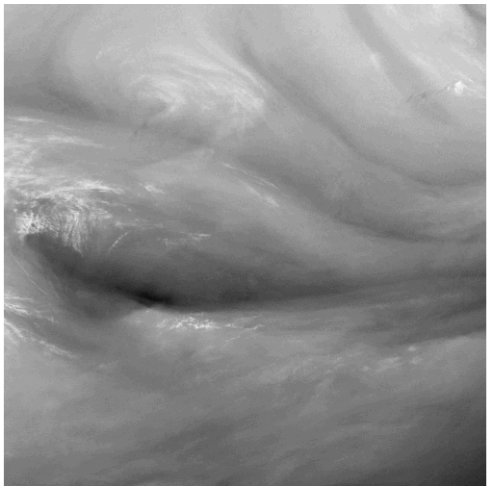

Figure 8 WV image around Japan scanned from 11:34:25AM to 11:39:16AM on March 18, 1997

ages at the location of the Fukuoka Meteorological Observatory was 6.67 km/pixel. The raw pixel values of the VS image (e.g., **Figure 6**), IR image (**Figure 7**), and WV image (**Figure 8**) are converted into albedo A_{VS} [-], equivalent black body temperature T_{bIR} [K] and T_{bWV} [K] respectively, by the calibration table attached to the each image. The albedo A_{VS} depends on the solar elevation angle h_s because it is defined as the ratio of the direct normal solar irradiance at the satellite to the irradiance reflected on the surface and received by the satellite. In this paper, the albedo A_{VS} is normalized to the normalized albedo A_{nVS} .

$$A_{nVS} = A_{VS} / \sin h_s \qquad (1)$$

The surface observed data and satellite observed data are combined together to be a database. The quality control procedure by the following criteria reduces the data sets from 8760 (= 365 x 24) to 2566,

(a) the solar elevation angle h_s beyond 5˚,

(b) A_{nVS} , T_{bIR} , T_{bWV} , I_{oG} , I_{oDN} and I_{oDH} are all valid.

The following multiple linear regression equations are examined to estimate hourly cumulative global irradiance I_{eG} [MJ/m^2] and hourly cumulative direct horizontal irradiance I_{eDH} [MJ/m^2].

$$I_{eG} = k_G + B_{G1} A_{nVS} + B_{G2} T_{bIR} + B_{G3} T_{bWV} + B_{G4} \sin h_s \quad (2)$$

$$I_{eDH} = k_D + B_{D1} A_{nVS} + B_{D2} T_{bIR} + B_{D3} T_{bWV} + B_{D4} \sin h_s \quad (3)$$

As the result of preliminary analysis, R square values were 0.826 for I_{eG} , and 0.591 for I_{eDH} . This suggested that further improvement be required for the I_{eDH} model.

Weather condition analysis

Figure 9 shows the scatterplot of the normalized albedo A_{nVS} with the equivalent black body temperature of IR image T_{bIR} . As shown in the legend, the visually observed cloud amount c_o classifies data plots under

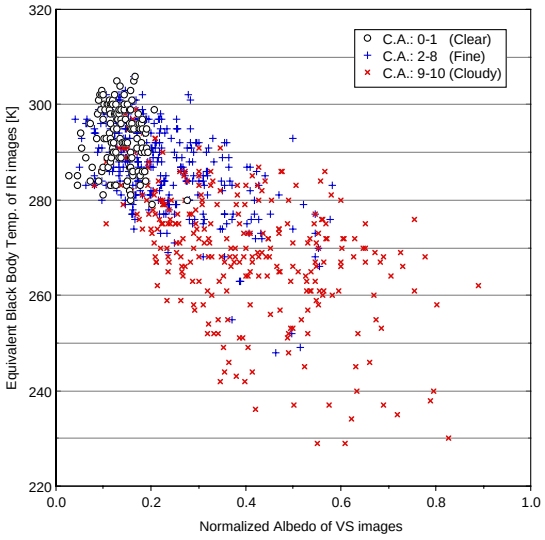

Figure 9 Scatterplot of Normalized Albedo of VS with Equvalent Black Body Temp. of IR

three weather conditions, i.e. *clear* (c_o =0,1), *fine* (c_o =2,3...8), and *cloudy* (c_o =9,10). This shows that plots for the *clear* sky condition are concentrated in the area, while plots for *fine* and *cloudy* conditions spread over the diagram. **Figure 10**, **Figure 11**, and **Figure 12** are the histgrams of the normalized albedo A_{nVS}, the equivalent black body temperature T_{bIR} and T_{bWV}, respectively. These diagrams shows that the normalized albedo A_{nVS} could be the most effective weather index which depends on the satellite image values.

Table 1 shows the percentiles and other basic statistics of the normalized albedo A_{nVS}. Because the 75% percentile in *clear* (c_o =0,1) condition is 0.159, and the 25% percentile in *fine* (c_o =2,3...8) condition is 0.145, the threshold between *clear* and *fine* is assumed to be 0.15. In the same manner, the threshold between *fine* and *cloudy* is assumed to be 0.25.

Table 1 Percentiles of Normalized Albedo of VS

	Surface Observed Cloud Amount			
	0-1	2-8	9-10	0-10
Valid cases	138	337	297	772
Minimum	0.027	0.041	0.081	0.027
Percentile (25%)	0.114	0.145	0.239	0.148
Percentile (50%)	0.135	0.192	0.362	0.214
Percentile (75%)	0.159	0.280	0.514	0.356
Maximum	0.277	0.582	0.890	0.890
Mean	0.136	0.222	0.383	0.268
Std.dev.	0.037	0.108	0.170	0.160

The database of 2566 cases is divided into three subsets according to the normalized albedo A_{nVS} :

(a) *Clear* (A_{nVS}≤0.15) 741 cases

(b) *Fine* (0.15< A_{nVS}≤0.25) 806 cases

(c) *Cloudy* (0.25< A_{nVS}) 1019 cases

The multiple linear regression analyses for the global irradiance and the direct horizontal irradiance are executed to three subsets of the database respectively using equations (2) and (3). As the results, partial regression coefficients for the multiple linear regression and R square values are shown in **Table 2**. The comparison of the measured global irradiance I_{mG} and estimated global irradiance I_{eG} are plotted in **Figure 13**. The measured direct horizontal irradiance I_{mDH} and estimated direct horizontal irradiance I_{eDH} are shown in **Figure 14**. **Table 3** summarizes the comparisons.

In Table 2, it is noted that the normalized albedo A_{nVS}, the equivalent black body temperature T_{bIR} and T_{bWV} are not always significant predictors of the irradiances, and the combinations of variables dependent on the weather condition. R square values of the global irradiance I_{eG} are acceptable for the weather conditions of *Clear* (R^2=0.866) and *Fine* (R^2=0.842). Those of I_{eG} for *Cloudy* (R^2=0.661) and direct horizontal irradiance I_{eDH} for *Clear* (R^2=0.660) would be on the margin for the applications of daylighting simulation. R square values of direct horizontal irradiance I_{eDH} for *Fine* (R^2=0.480) and *Cloudy* (R^2=0.301) would be inapplicable to the simulations.

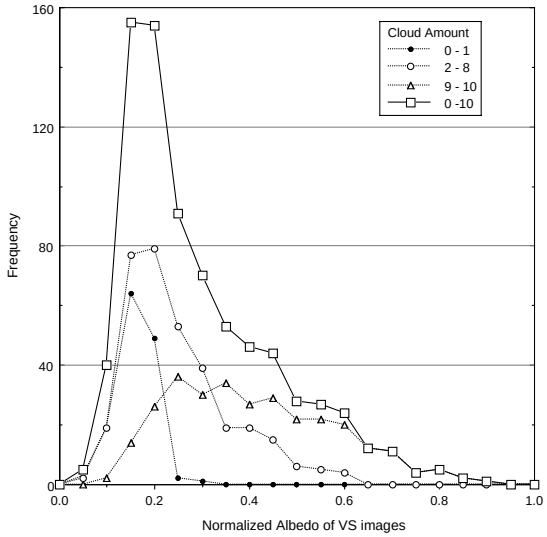

Figure 10 Histgram of Normalized Albedo of VS images

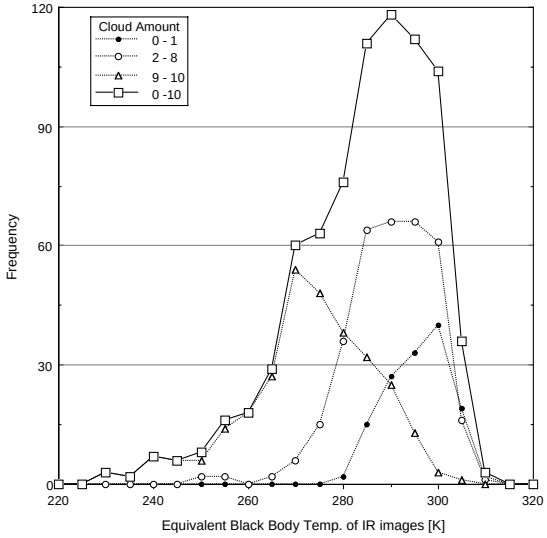

Figure 11 Histgram of Equvalent Black Body Temperature of IR images

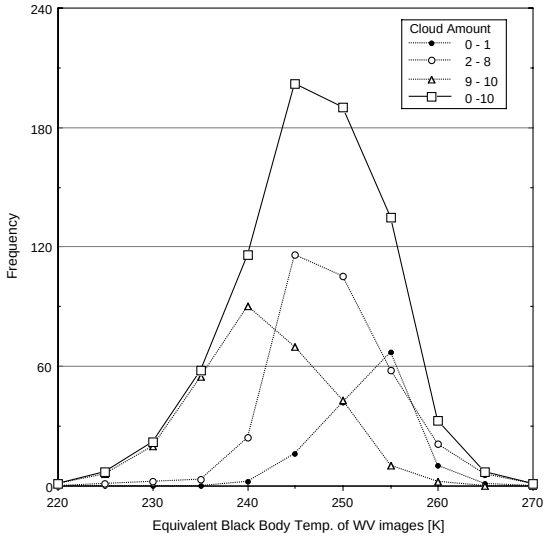

Figure 12 Histgram of Equvalent Black Body Temperature of WV images

Table 2 Coefficients of Multiple Regression Models

Model [MJ/m²h]		k	B_1	B_2	B_3	B_4	Cases	R^2	F	Sig.
Global Irradiance	Clear	8.89E-2	-2.70E+0	0	0	3.65E+0	741	0.866	2.39E+3	.0000
	Fine	-2.32E+0	-2.99E+0	0	1.05E-2	3.44E+0	806	0.842	1.43E+3	.0000
	Cloudy	-2.73E-1	-1.89E+0	3.43E-3	0.00E+0	2.25E+0	1019	0.661	6.61E+2	.0000
Direct Horizontal Irradiance	Clear	-6.44E+0	0	0	2.47E-2	2.50E+0	741	0.660	7.16E+2	.0000
	Fine	-3.71E+0	-5.04E+0	0	1.80E-2	1.99E+0	806	0.480	2.47E+2	.0000
	Cloudy	-1.44E+0	-9.53E-1	6.37E-3	0	7.43E-1	1019	0.301	1.46E+2	.0000

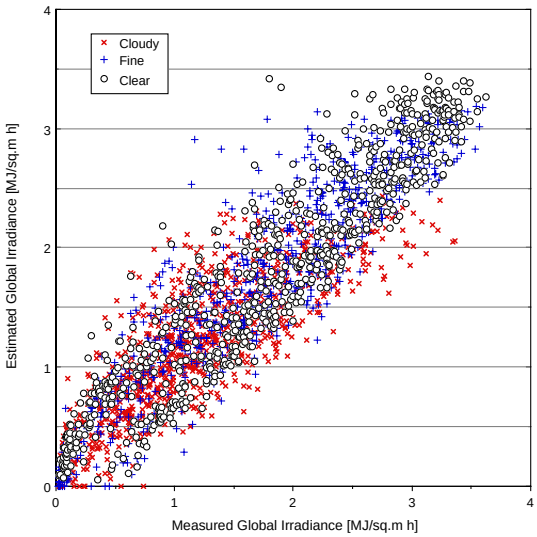

Figure 13 Scatterplots of Measured and Estimated Global Irradiance

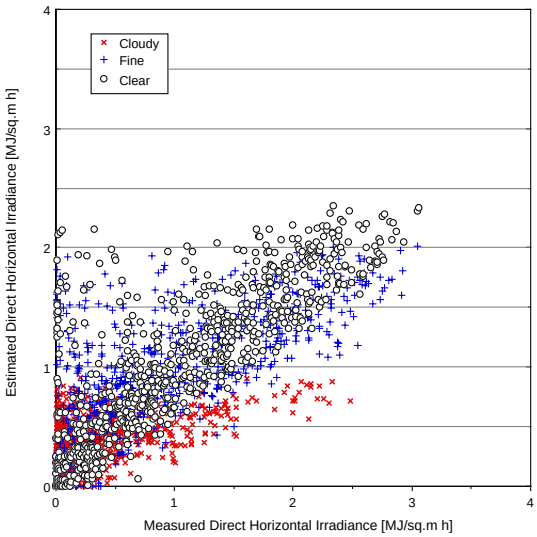

Figure 14 Scatterplots of Measured and Estimated Direct Horizontal Irradiance

Table 3 Comparison of Measured and Estimated Irradiance

[MJ/m²h]	Measured		Estimated	
	Global	Direct Horizontal	Global	Direct Horizontal
Cases	2566	2566	2566	2566
Minimum	0.020	0.001	0.000	0.000
Maximum	3.620	3.062	3.435	2.346
Average	1.551	0.731	1.552	0.737
Std.Dev.	0.897	0.739	0.811	0.571
RMSE			0.374	0.455
MBE			0.001	0.006

In short, the more clouds cause the less correlation. One major reason would be that the surface observed irradiance values are hourly cumulative global irradiance, while a pixel value on the satellite image is measured instantaneously by the satellite that rotates in 100 revolutions per minute. A method to improve the correlation with the cumulative irradiance is to utilize the average of surrounding pixels instead of one pixel which corresponding the location [3]. Unfortunately, this is less useful for the daylighting simulation, because instantaneous global and direct illuminance values are required as well as the cumulative values. The better solution would be the utilization of surface observed instantaneous global and direct illuminance data that synchronized with the satellite scanning.

Daylight source model

For the daylighting simulation, the instantaneous data of diffuse illuminance and direct horizontal illuminance for the specific time and location are usually required. The satellite derived global and direct horizontal irradiance values I_G and I_{DH} are converted into the diffuse illuminance E_d [lx] and the direct horizontal illuminance E_{DH} [lx] by the luminous efficiency of sky light η_d and sun light η_D [10] on the assumption that the instantaneous data is equal to the average in the period.

$$\eta_O = I_O / E_O$$

$$\eta_d = \eta_O(3.375\sin^3 h_s - 6.175\sin^2 h_s + 3.471\sin h_s + 0.7623) \quad (4)$$

$$\eta_D = \eta_O\{(6.25\sin^3 h_s - 10\sin^2 h_s + 3.94\sin h_s) I_{DN} / I_O + 0.983\sin h_s + 0.451\} \quad (5)$$

$$E_d = \eta_d (I_G - I_{DH}) \quad (6)$$

$$E_{DH} = \eta_D I_{DH} \quad (7)$$

Daylight performance simulation

The daylight source model based on the meteorological satellite images mentioned above and the satellite image database for one year from July 1996 through June 1997 are linked with the daylight simulation program [11].

The program has capabilities as a flexible daylighting simulation tool for designers, engineers, and researchers. It handles any shape of architectural space as long as composed of polygons. Reflection properties of the building materials are specified by the bidirectional reflection function that models isotropic diffuse, anisotropic diffuse, or specular . The interreflection of light is described by the integral equation and solved numerically. As daylight source, direct solar illuminance, diffuse illuminance, and/or sky luminance distribution can be selected. The simulated results are output numerically and graphically as the spatial distributions of illuminance and luminance.

Linking with the satellite derived daylight source model and the satellite image database, not only spatial distribution but temporal distribution of light has become possible to be simulated.

The simulation system is applied to the model room shown in **Figure 15**. **Figure 16** shows the spatial distribution of the illuminance on the floor under following condition,

Location:	Fukuoka
Date:	June 1, 1997
Time:	11:37AM
Solar altitude:	77.9˚
Solar azimuth:	-17.3˚
A_{nVS}	0.190
T_{bIR}	280 [K]
T_{bWV}	236 [K]
E_d	52402 [lx]
E_{DH}	58115 [lx].

Figure 16 shows the temporal distribution of the illuminance. At 11:37 AM on the every first day of the month from July 1st 1996 through June 1st 1997, the diffuse and direct horizontal illuminance E_d and E_{DH} , and the illuminance at the center of the floor of the model room are estimated.

CONCLUSIONS

A new statistical model to estimate global and direct irradiance and illuminance using geostational meteorological satellite images is developed. The illuminance model and a satellite image database for a year is linked to daylight simulation program. The combination of the satellite derived solar daylight source model and the daylighting simulation program demonstrated that not only spatial distribution but temporal trend of illuminance in building environment is able to be estimated.

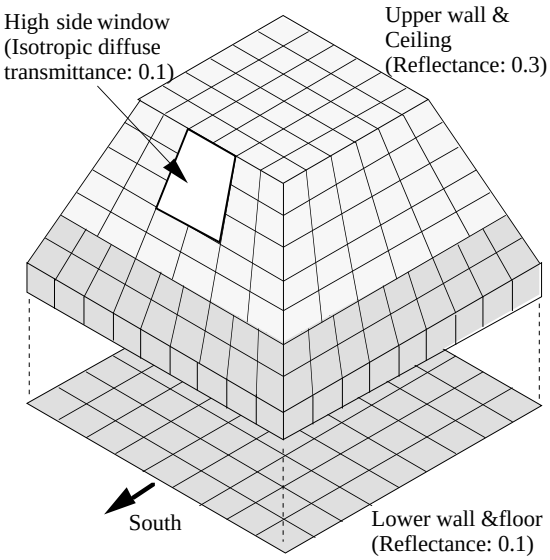

Figure 15 Simulated model room

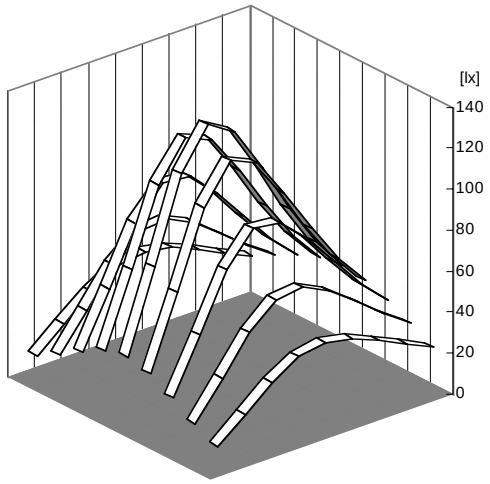

Figure 16 Illuminance distribution on the floor at 11:37AM June 1, 1997 in Fukuoka

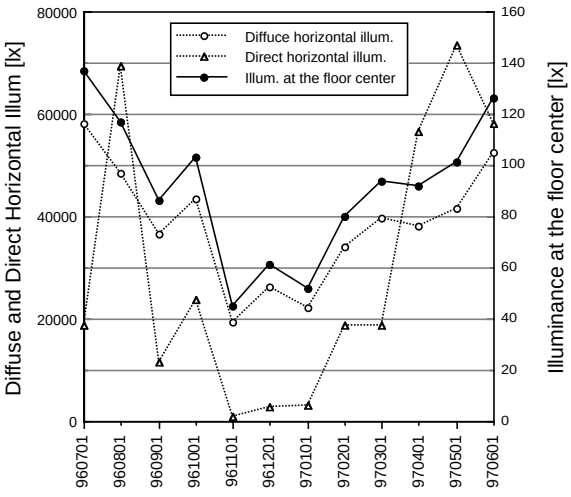

Figure 17 Variation in the floor illuminance at 11:37 AM of the first day of every month

The further study is expected using instantaneously observed global and direct irradiance and illuminance data for the improvement and validation of the model.

ACKNOWLEDGMENTS

This work was supported by the Grant-in-Aid of the Ministry of Education, Science and Culture 1998, and the Iwatani Naoji Memorial Fund 1998. The image processing was performed using the public domain NIH Image program written by Wayne Rasband at the U.S. N.I.H.

REFERENCES

1. Tarpley J. D., ''Estimating incident solar radiation at the surface from geostationary satellite data'', J. Applied Meteorology, Vol.18, pp.1172-1181, 1979.
2. Gautier C., Diak G. and Masse S., ''A simple physical model to estimate incident solar radiation at the surface from GOES satellite data'', J. Applied Meteorology, Vol.19, pp.1005-1012, 1980.
3. Cano D., Monget J. M. , Albuisson M., Guillard H., Regas N. and Wald L., ''A Method for the Determination of the Global Soar Radiation from Meteorological Satellite Data'', Solar Energy, Vol.37, No.1, pp.31-39, 1986.
4. Diabate L., Demarcq H., Regas N. and Wald L, ''Estimating incident solar radiation at the surface from images of the earch transmitted by geostationary satellites: the Heliosat project'', Int. J. Solar Energy, Vol.5, pp.261-278, 1988.
5. Perez R., Seals R., Stewart R., Zelenka A., Astrada-Cajikal V., ''Using satellite-derived insolation data for the site/time specific simulation of solar energy systems'', Solar Energy, Vol.53, No.6, pp.491-495, 1994.
6. Fontoynont M., Dumortier D. et al., ''Satellight: a European programm dedicated to serving daylight data computed from Meteosart images'', Lux-Europa Conference, Amsterdam, pp.1-12.1997.
7. Uetani Y., ''Prediction of the Global and Direct Irradiance and Illuminance by the Geostational Meteorological Satellite Images'', Proceedings of the 24th Session of the CIE, Warsaw, June 24-30, 1999 (in print).
8. Kidder S. Q. and Vonder Haar T. H., ''Satellite Meteorology-an Introduction'', Academic Press, 1995.
9. JMBSC, ''The Meteorological Satellite Monthly Report'', July 1996 - June 1997.
10. Kimura K., Kentiku Kankyo-Gaku 1, Maru-zen, 1992 (in Japanese).
11. Uetani Y. and Matsuura K., ''A Method of Luminance Calculation in an Anisotropic Diffuse Reflecting Interior'', Journal of the Illuminating Engineering Society, Vol.22, No.2, pp.162-175, 1993.

NOMENCLATURE

I_{oG} Surface observed hourly cumulative global irradiance [MJ/m^2]

I_{oDN} Surface observed hourly cumulative direct normal irradiance [MJ/m^2]

I_{oDH} Surface observed hourly cumulative direct horizontal irradiance [MJ/m^2]

c_o Visually observed cloud amount, [-]

A_{VS} Albedo derived from VS image, [-]

A_{nVS} Normalized albedo derived from VS image, [-]

T_{bIR} Equivalent black body temperature derived from IR image, [K].

T_{bWV} Equivalent black body temperature derived from WV image, [K].

h_s Solar elevation angle, [˚].

I_{eG} Estimated hourly cumulative global irradiance [MJ/m^2].

I_{eDH} Estimated hourly cumulative direct horizontal irradiance [MJ/m^2].

k_G , B_{G1} , B_{G2} , B_{G3} , B_{G4} Constant and partial regression coefficients in the multiple linear regression equation for I_{eG} .

k_D , B_{D1} , B_{D2} , B_{D3} , B_{D4} Constant and partial regression coefficients in the multiple linear regression equation for I_{eDH} .

I_O Solar constant, 1353 [W/m^2].

E_O Solar illuminance constant, 127000 [lx].

I_{eDN} Estimated instantaneous direct normal irradiance [W/m^2].

η_d Luminous efficiency of the sky light [lm/W].

η_D Luminous efficiency of the sun light [lm/W].

E_d Diffuse illuminance [lx].

E_{DH} Direct horizontal illuminance [lx].